LIMNOLOGY and OCEANOGRAPHY: METHODS

ASLO

Limnol. Oceanogr.: Methods 21, 2023, 615–624

doi: 10.1002/lom3.10569

Digitizing lake bathymetric data using ImageJ

Christopher I. Rounds [1]*, **Kelsey Vitense** [1,a], **Gretchen J. A. Hansen** [1]

[1]Department of Fisheries, Wildlife, and Conservation Biology, University of Minnesota, St. Paul, Minnesota, USA

Abstract

Lake morphometry is a driver of limnological processes, yet digitized bathymetry is lacking for most lakes. Here, we describe a method for efficiently extracting hypsography from bathymetric maps using ImageJ. To validate our method, we compared results generated from two independent users to those obtained from digital elevation models for 100 lakes. The mean absolute difference between hypsographic curves extracted using ImageJ vs. digital elevation models (DEMs) was 0.049 (95% CI 0.041–0.056) proportion of lake area, suggesting that ImageJ provides accurate hypsography. We calculated the mean absolute difference between the two users (0.016; 95% CI: 0.011–0.021), which suggests high interobserver reliability. Finally, we compared DEMs to an interpolated hypsography using only the maximum lake depth and found large differences. We apply this method to extract data for 1012 lakes. Our data and approach will be useful where bathymetric maps exist but are not digitized.

Lake morphometry (i.e., lake depth, area, and volume) is an important driver of chemical and biological properties in lakes. Morphometry impacts almost all transport processes in lakes, including sedimentation, resuspension, mixing, and burial of lake substances (Carpenter 1983; Håkanson 2005). Lake area and depth are also important in determining a lake's thermal regime (Stefan et al. 1996; Pal'shin et al. 2008; Winslow et al. 2015). The thermal regime influences duration and strength of stratification, which consequently regulates oxygen levels and oxygen depletion events (Gorham and Boyce 1989; Håkanson 2004). In addition, a lake's depth profile in part determines volume, which alters water retention time and in-lake processes such as primary production and nutrient retention (Carpenter 1983; Kalff 2002; Algesten et al. 2004).

Despite the importance of depth for limnological processes, lake-rich landscapes often lack even the most basic information on depth. For example, of the 479,950 lakes with a surface area over 4 ha in the coterminous United States, maximum depth data are available for only 17,765 lakes (3.7%), and mean depths are available for only 1360 lakes (0.28%) (Stachelek et al. 2021). Lake depth data are required for landscape-level models of lake temperature (Rose et al. 2016; Winslow et al. 2017), deep-water dissolved oxygen (Jacobson et al. 2010), total phosphorus (Cross and Jacobson 2013), and cold-water fish habitat (Herb et al. 2014).

The dearth of information on lake morphometry has led to several efforts to predict lake morphometric characteristics (e.g., maximum depth, mean depth, and volume). Studies have predicted morphometry from different combinations of catchment and lake characteristics (e.g., local slope, lake surface area, lake perimeter, maximum depth, and in-lake distance from the shoreline) with mixed results (Hollister and Milstead 2010; Hollister et al. 2011; Sobek et al. 2011; Heathcote et al. 2015; Oliver et al. 2016). Recent efforts have focused on calculating and providing these data globally (Messager et al. 2016; Khazaei et al. 2022). The most powerful mean depth predictor is generally local slope (Sobek et al. 2011; Heathcote et al. 2015), but the relationship between mean depth and slope is insufficient (R^2 of 0.31–0.52) for many practical applications (Sobek et al. 2011; Heathcote et al. 2015). A simple method to derive morphometric variables is to assume a consistent lake shape (for more discussion, *see* Hollister and Milstead 2010), which is often done by using maximum lake depth to calculate hypsography (Read et al. 2014; Winslow et al. 2017). Recent work has suggested remote sensing and LIDAR can be accurate measures of depth but most work has been done in shallow waters, and equipment can be cost prohibitive (Schwarz et al. 2019; Ai et al. 2020).

*Correspondence: round060@umn.edu

Author Contribution Statement: C.I.R. developed methods, conducted analyses, and wrote the paper. K.V. developed methods, conducted analyses, and edited the paper. G.J.A.H. developed the idea, obtained funding, and edited the paper.

Additional Supporting Information may be found in the online version of this article.

[a]Present address: Scientific Computing and Data Curation Division, U.S. Environmental Protection Agency, Duluth, Minnesota, USA

Lake morphometry is generally measured using echo sounding and visualized using bathymetric contour maps (Fig. 1A). Currently, consumer-grade depth finders can produce high-quality bathymetric maps (Dost et al. 2008), but digitized data produced by most consumer software are protected by copyright and not readily available to researchers. To enable the calculation of basic limnological variables (e.g., mean depth, volume, proportion littoral, water residence time), paper (or PDF) bathymetric contour maps can be digitized and georeferenced to create digital elevation models (DEMs), which provide gridded values of lake depth at regularly spaced intervals. These DEMs can be summarized as lake hypsography (i.e., lake area at or below various depths), and hypsographic curves can be used to calculate lake volume and other relevant variables (Fig. 1B). Unfortunately, obtaining or producing hypsographic data can be difficult because bathymetric data are often only available in unpublished tables and agency paper maps, and creating georeferenced DEMs requires substantial time and expertise. These limitations have led to a deficiency in lake depth data over broad spatial extents (Stachelek et al. 2021).

The goal of this project was to develop a method for accurately and rapidly digitizing hypsographic data. We used the open-source image processing software ImageJ (Rueden et al. 2017) to extract hypsographic information from publicly available bathymetric maps. Using this method, we were able to build a hypsographic dataset quickly and accurately for lakes across Minnesota, South Dakota, and Wisconsin, U.S.A. (Rounds et al. 2022). To assess the accuracy of our method, we calculated mean absolute difference of ImageJ-derived hypsographic data relative to hypsographic data extracted from spatially georeferenced DEMs. To show that ImageJ-derived hypsography is replicable across users, we calculated mean absolute difference between hypsographic data from two independent processors. In addition, we calculated mean absolute difference of hypsography generated by assuming a consistent lake basin shape and known maximum depth to compare with the accuracy of ImageJ-derived hypsography. Finally, we compare the lake volume calculated from DEMs to ImageJ and hypsography generated by assuming a consistent lake basin shape. We present here both the hypsographic data and the method for extracting such data from bathymetric maps to enable other researchers to employ similar approaches to increase the availability of lake morphometric data globally.

Materials and procedures

Digitizing bathymetric maps with ImageJ

We obtained bathymetric maps as PDFs from the state agencies in Minnesota, South Dakota, and Wisconsin. These maps are a historical dataset on lake depth characteristics. We consulted with state agency data managers to ensure we obtained the most complete and up-to-date set of bathymetric maps. The scale of the maps varies greatly between lakes with the scale being directly related to lake surface area.

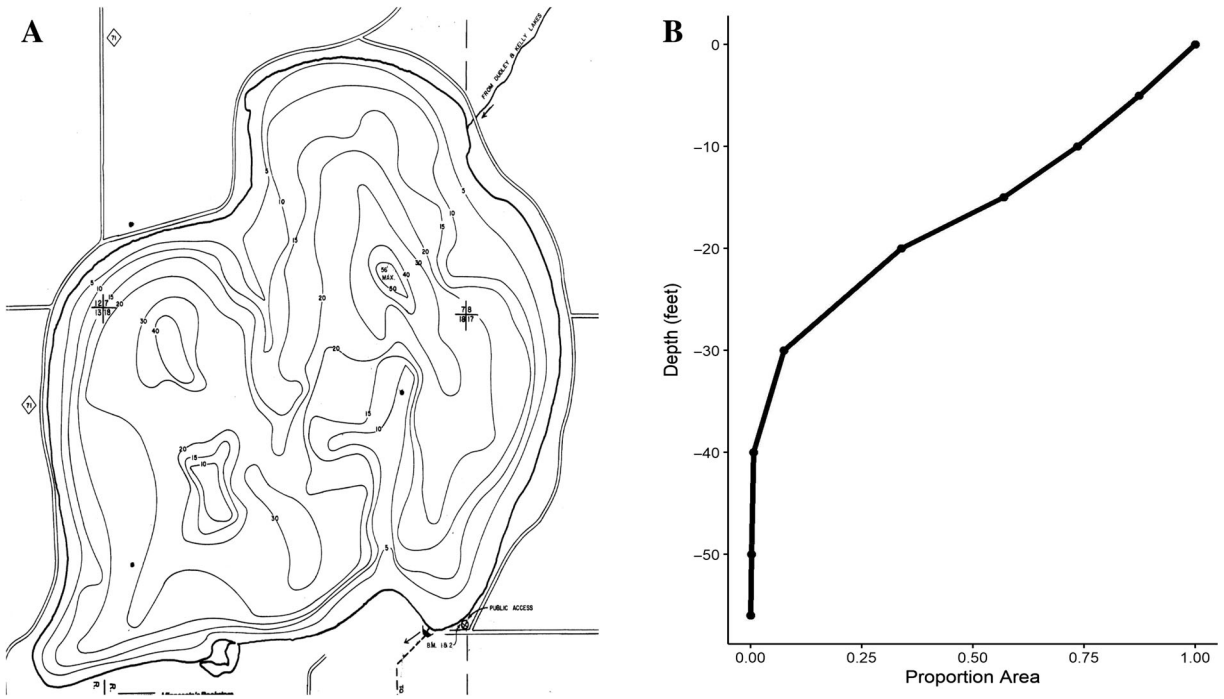

Fig. 1. Conceptual diagram showing a bathymetric map (**A**) and a hypsographic curve for the map (**B**). Notice the hypsographic curve starts in the upper right corner with all of the lake at 0 ft and the proportion area decreases until there is no lake area at the maximum depth of 56 ft.

Contour intervals for these maps were most commonly 5 ft, but in some instances, lakes had contour intervals at 1, 3, 5, or 10 ft.

Initial preprocessing was necessary before we were able to extract data from bathymetric maps. After obtaining the maps, we converted PDF files to TIFF files. Individual lake image files were imported into ImageJ and examined for completeness. Most lakes required modifications to the contour lines because ImageJ can only measure polygons that are fully enclosed. Using the Drawing tool, we filled breaks in all contour lines to create complete polygons (the tool allowed us to draw in new segments; Supporting Information Fig. 1). This step was completed for each contour line until every contour was a fully enclosed polygon. In some instances, contour lines would touch other contour lines, in which case we used the Erase tool (allowing us to erase overlapping segments) followed by the Drawing tool to create separate contour lines (Supporting Information Fig. 2).

After initial preprocessing, we measured the areas inside contour lines in square pixels. If the maximum depth of a lake was represented by a point (and not a contour interval), we recorded that depth as having zero area. Once we had the area inside each contour line, we divided each area by the total surface area of the lake (in square pixels). The result is proportional areas of the lake between contour lines. Lake hypsography was then calculated as the cumulative proportion of lake area at or below the depth of each contour line ("below" meaning "at greater depth"). Multiplying these proportional areas by the surface area of the lakes gives physical areal units of hypsography. A step-by-step video tutorial can be found accompanying the dataset (Rounds et al. 2022) and more specific methods can be found in the Supporting Information.

Accuracy and agreement of ImageJ hypsography

We validated the results of ImageJ-derived hypsography in three ways. First, we calculated the mean absolute difference (MAD) and mean signed difference (MSD) between hypsography we digitized with ImageJ and fully digitized hypsography from DEMs for a subset of 100 lakes. Second, we evaluated the reproducibility of this method by comparing the MAD and MSD between two separate ImageJ users. Third, we created null hypsography by using lake maximum depth and assuming a consistent lake depth profile (i.e., area of a lake decreases linearly with depth) and calculated the MAD and MSD between null hypsography and hypsography derived from DEMs. We then used these metrics to compare the relative performance of ImageJ-derived hypsography vs. null hypsography in approximating the DEM hypsography. To contextualize our work, we calculate symmetric mean absolute percent error (SMAPE) between DEM-derived volume and volume derived from ImageJ and null hypsography.

We assessed the accuracy of hypsography extracted from bathymetric maps using ImageJ by comparing our results to hypsography from fully digitized, spatially referenced bathymetric maps available as DEMs from the Minnesota Department of Natural Resources ((https://gisdata.mn.gov/dataset/water-lake-bathymetry, last accessed August 2020). The test of agreement was done by randomly selecting 100 Minnesota, U.S.A. lakes for which high-resolution DEMs of lake depth were available. Two users digitized the 100-lake set separately using the ImageJ methods described above and without knowledge that depth data existed for these lakes. For these 100 lakes, we converted the DEMs to raster data using the R package "raster" (Hijmans and van Etten 2012), computed cumulative lake areas at depth (typically at 1 ft depth intervals), and converted physical areas to proportional areas by dividing by lake surface area. We then compared each DEM and ImageJ hypsographic curve using proportional area over the full range of depths covering both curves. The area-at-depth relationships were linearly interpreted at 0.1 ft intervals (from 0 to the largest maximum depth of the digitizations) for both curves so that area could be compared at the same depths. Agreement between ImageJ and DEM hypsography was quantified by calculating the MAD in proportional area, defined by the equation

$$\mathrm{MAD}_j = \frac{\sum_{i=1}^{N_j} \left| \left(Digitized_{i,j} - DEM_{i,j} \right) \right|}{N_j} \quad (1)$$

where $N_j = D_j/\Delta d$ is the number of depth contours for lake j, D_j is the maximum depth of lake j (largest of the ImageJ or DEM maximum depths, rounded to one decimal place), Δd is the depth resolution after interpolation (set to 0.1 ft), $\mathrm{Digitized}_{i,j}$ is the interpolated lake area from the digitized ImageJ curve at depth i for lake j, $\mathrm{DEM}_{i,j}$ is the interpolated lake area from the DEM curve at depth i for lake j. For lakes with high levels of disagreement (MAD >0.1 proportion of lake area), hypsographic curves were compared visually to determine reasons for differences. We also calculated the MSD between the hypsographic data from ImageJ and the DEMs in order to determine the directionality of observed differences. The MSD is calculated in the same way as MAD but without the absolute value in the numerator.

To determine how different users impact the accuracy of ImageJ digitization we calculated the MAD and MSD using the hypsography digitized by two different ImageJ processors.

$$\text{Interobserver MAD}_j = \frac{\sum_{i=1}^{N_j} \left| \left(Processor\ One_{i,j} - Processor\ Two_{i,j} \right) \right|}{N_j} \quad (2)$$

The equation for interobserver MAD uses the same notation as defined in Eq. 1, where the same interpolations were used as in the ImageJ vs. DEM comparison above. This calculation is similar to the MAD, but we are comparing ImageJ processor performance instead of differences between ImageJ digitizations and DEMs.

To determine how previous assumptions of lake depth compare to the accuracy of ImageJ digitizations we calculated MAD and MSD for a "null hypsography" method. We utilized the generate_hypsography() function from the R package "glmutils" (Stachelek 2022) to generate null hypsographic models based only on the maximum depth of a lake. This function estimates lake area at each depth using a linear interpolation of maximum depth, sometimes known as the cone method (Hollister and Milstead 2010). While generating null hypsography we used the maximum depth from the DEMs, the same number of layers as the DEM maximum depth, and only included results from the linear interpolation of maximum depth (all input variables for the generate_hypsography function). It should be noted that an ellipsoid interpolation of max depth is also available in glmutils, but MAD for the ellipsoid interpolation was consistently double that of the linear

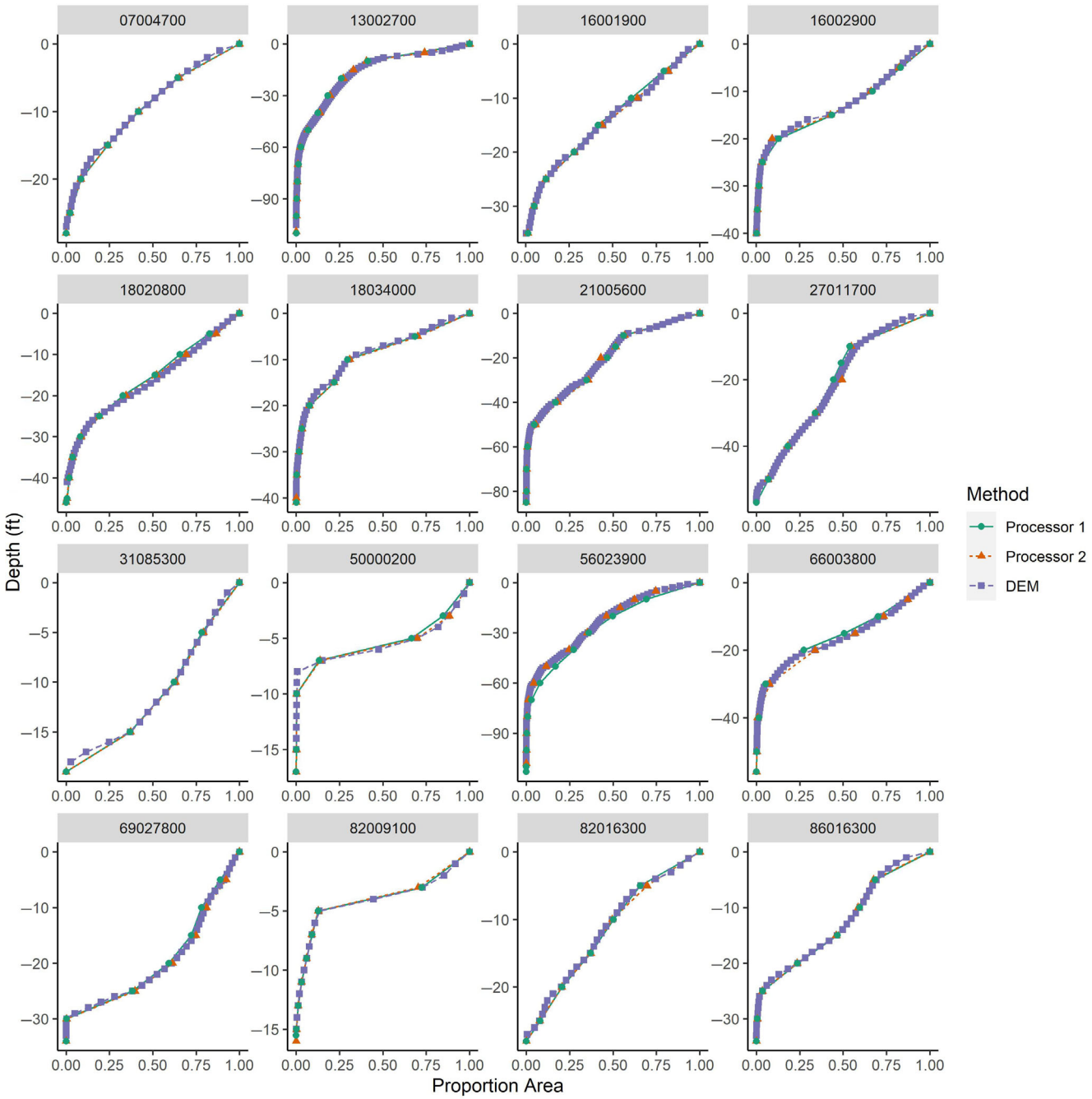

Fig. 2. Hypsographic curves for example lakes showing high levels of agreement (mean absolute difference <0.015) between hypsography generated from ImageJ and the lake digital elevation models. Panel titles indicate lake identifiers.

interpolation (average MAD = 0.38 proportion of lake area). We compared the MAD and MSD calculated from the null hypsographic curves vs. the DEM to the MAD and MSD calculated from ImageJ digitizations vs. the DEM. This comparison shows the differences in accuracy between a method that has been used previously and digitizing bathymetry using ImageJ.

To assess how lake volume calculations differed between DEMs and the ImageJ and null hypsography we calculated the volume of each lake following Kalff (2002). To compare the difference in calculated volume between the DEMs and ImageJ, we calculated SMAPE, given by

$$\mathrm{SMAPE}_{i,j} = 100 \times \frac{1}{n} \sum \frac{|\,\text{Reference volume}_j - \text{Digitized volume}_{i,j}\,|}{\left(\text{Reference volume}_j + \text{Digitized volume}_{i,j}\right)/2} \quad (3)$$

where i refers to method i (with method being either ImageJ processor 1, ImageJ processor 2, or the null hypsography), j refers to lake j and n is the number of lakes in the set. Reference volume is the volume calculated for the DEM. SMAPE is a value reflecting how close two measurements are to each other with small values indicating more similar measurements

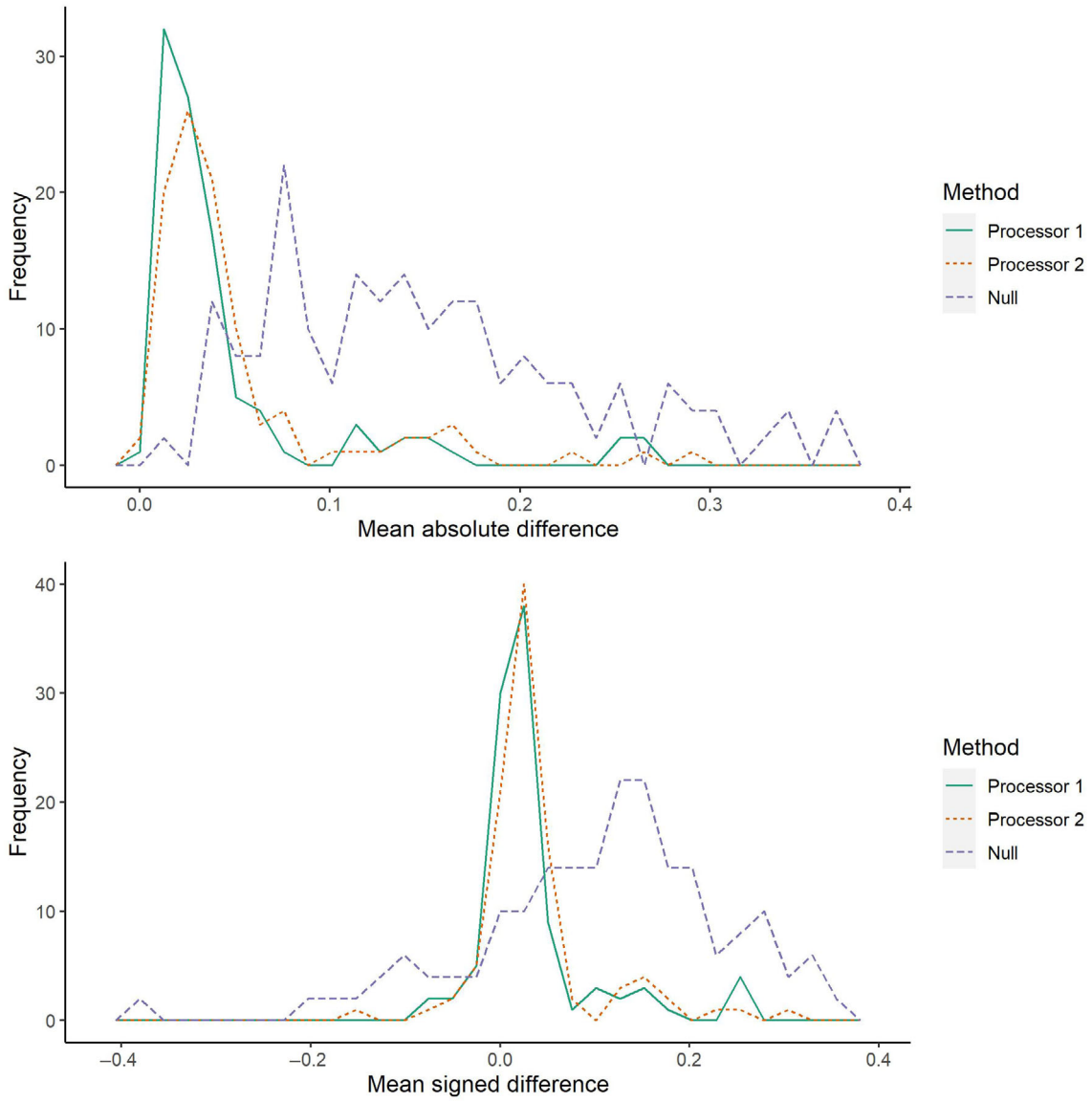

Fig. 3. (**A**) MAD between hypsographic curves generated from ImageJ or the null hypsography vs. DEMs for 100 validation lakes. Smaller values indicate higher agreement. (**B**) MSD between the hypsographic data generated from ImageJ or the null hypsography vs. DEMs. Values above zero indicate the method is estimating larger lake area on average across the depth ranges compared to the DEM.

and large values indicating measurements that are further apart. We also calculated the lake volume SMAPE for the two ImageJ processors (by using processor 1 as the reference volume in Eq. 3) to determine how volume calculations differed between users.

Assessment

In our analysis of 100 lakes across Minnesota, we found high agreement between hypsographic curves generated using ImageJ and those generated from lake DEMs (Fig. 2). The average MAD between ImageJ and DEM hypsographic curves across lakes was 0.046 proportion of lake area (95% CI: 0.035–0.057; Fig. 3A) for processor 1 and 0.051 (95% CI: 0.040–0.062; Fig. 3A) for processor 2. The average MSD across lakes was 0.033 proportion of the total lake area (95% CI: 0.021–0.046; Fig. 3B) for processor 1 and 0.037 for processor 2 (95% CI: 0.024–0.050; Fig. 3B). There were instances of noticeable differences in the hypsography generated from bathymetric maps and lake DEMs, with 14 lakes having MAD >0.1 (Fig. 3A; Table 1). However, most of the hypsographic curves matched well, with MAD <0.05 for 78% of lakes.

The comparison between the two ImageJ processors had high agreement indicating the ImageJ's inter-observer reliability. The average MAD from the two processors was 0.016 proportion of lake area (95% CI: 0.011–0.021). The average MSD was similarly small at −0.004 proportion of lake area (95% CI: −0.010–0.002). In this comparison there were three lakes for which inter-observer MAD exceeded 0.1. These differences were the result of user error while digitizing (Table 1—Reason behind Disagreement = User error).

The hypsographic curves generated by using maximum lake depth and assuming a linear interpolation of depth (the null hypsography) differ from DEM hypsography substantially more than the ImageJ approach (Fig. 3). The average MAD of the null hypsography was 0.150 proportion of total lake area (95% CI: 0.134–0.167; Fig. 3A). In total, 9% of the null hypsographic curves had a MAD <0.05 proportion of total lake area. In addition, the average MSD of the null model was also much higher than that reported for ImageJ (0.108 proportion of total lake area, 95% CI: 0.082–0.134; Fig. 3B).

The volume calculations between ImageJ and the DEMs were highly similar and replicable between users while volume calculations from the null hypsography was less accurate. The SMAPE for the 100 lake set with the DEMs and processor 1 was 10.8% while processor 2 had a SMAPE value of 12.3%. The between ImageJ user SMAPE was calculated to be 3.7% highlighting the replicability between users. The SMAPE for the null hypsography compared to the DEMs had a much larger SMAPE value of 35.3% indicating much poorer performance from the null model compared to ImageJ digitizations.

Discussion

We present a new method for rapidly and accurately digitizing lake bathymetric information and extracting hypsography using the open-source software ImageJ. To assess the accuracy of ImageJ digitizations of bathymetric maps, we calculated differences between DEM and ImageJ hypsographic curves. We found that hypsography matched well between the approaches with an average MAD of 0.049 proportion of lake area. To determine interuser replicability, we calculated differences between hypsographic curves generated from two different ImageJ users. In this case, MAD between users was low, at 0.016 proportion of lake area. We also calculated differences between DEM and null hypsography. We found the null

Table 1. Explanation of discrepancies between hypsography measurements generated from ImageJ and from digital elevation models for lakes with a MAD > 0.1. Minnesota DNR lake ID (DOW), lake name, lake county, and MSD are also given. MAD and MSD are averages between both processors.

DOW	Lake name	County	Reason behind disagreement	MAD	MSD
03048400	Ellison	Becker	User error	0.151	0.151
11011700	Twenty-six	Cass	Difference between maps	0.160	0.160
13005400	Little comfort	Chisago	Difference between maps	0.111	0.086
30014300	N. Stanchfield	Isanti	User error	0.170	0.170
33003600	Fish	Kanabec	Few contour lines, difference between maps	0.209	0.209
38053900	Cloquet	Lake	Few contour lines, difference between maps	0.138	0.138
47006400	Erie	Meeker	Difference between maps	0.116	0.116
58014200	Pokegama	Pine	Difference between maps	0.127	0.127
61007800	Reno	Pope	Difference between maps	0.167	0.168
69004400	Butterball	St. Louis	Few contour lines	0.214	0.214
69039700	Clearwater	St. Louis	Difference between maps	0.144	0.144
69074200	Ban	St. Louis	Difference between maps	0.279	0.279
71004600	Diann	Sherburne	Few contour lines	0.261	0.261
86024200	Wiegand	Wright	User error	0.156	−0.156

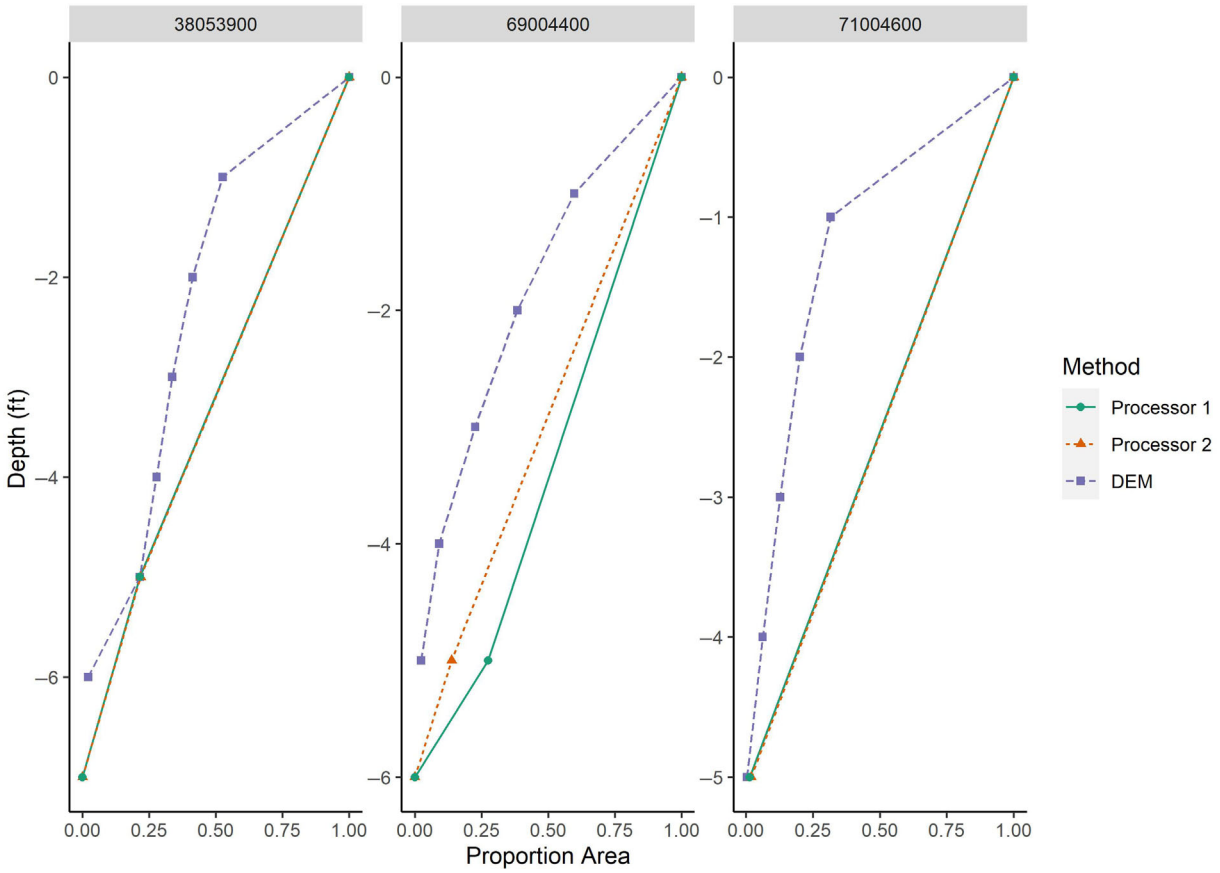

Fig. 4. Relative hypsographic curves for shallow lakes with few contours. The hypsographic curves differ due to the difference in the spatial resolution of the original bathymetric maps and the spatially interpolated DEMs, as well as differences in maximum depth.

hypsography to be substantially less consistent with DEM-derived hypsography and volume, with an average MAD of 0.150 proportion of lake area. Although our method relies on the use of existing bathymetric maps, we believe using ImageJ to digitize existing bathymetric maps will greatly increase the number of lakes for which area-at-depth measurements exist.

Hypsography generated from ImageJ differed from digital elevation models for three main reasons (Table 1). Differences were most commonly due to actual discrepancies between the two data sources (9 of 14 lakes). In some cases, maximum depths recorded on the scanned historical bathymetric maps and DEMs differed (differences in *y*-intercepts in Fig. 4). In other cases, differences in the resolution of the contour lines of the maps produced differences in hypsography. Low resolution or few contour lines influenced data quality in four lakes, all of which had a maximum depth of less than 12 ft. These shallow lakes had a relatively high MAD because bathymetric maps only had contour lines every 5 ft (sometimes every 10 ft), resulting in a small number of contours available for measurement in ImageJ. The low-resolution hypsographic curves produced using ImageJ contrast with the higher-resolution depth data produced through spatial interpolation in the DEM. Even if the areas at the contour lines match the corresponding areas in the DEM, there is still likely to be a difference in the shape of the hypsographic curves because of the spatial interpolation used when creating the DEM (e.g., Fig. 4). Finally, hypsography for three lakes differed due to user error in digitization, particularly for multi-basin lakes. In these instances, the user digitized the wrong lake or portion of a lake that was present on the same PDF document.

The MSD calculation indicates the directionality of the differences between hypsographic curves. Integrating a lake hypsographic curve gives lake volume. Thus, the positive MSD calculated for ImageJ implies that the estimate of lake volume from the digitized map will be larger than the lake volume estimate from the DEM. From the comparison of the bathymetric maps and DEMs, we found that a contributing factor to this phenomenon is that the maximum depth of the bathymetric maps was often greater than the maximum depth of the DEM. Seven of the nine lakes with differences in maximum depths had a bathymetric map with a greater maximum depth than the DEM. The null hypsographic curves had even higher MSDs than ImageJ, indicating the null approach estimates lakes to have greater volumes than ImageJ.

The MAD and MSD calculated between the two ImageJ processors was low indicating high inter-observer reliability.

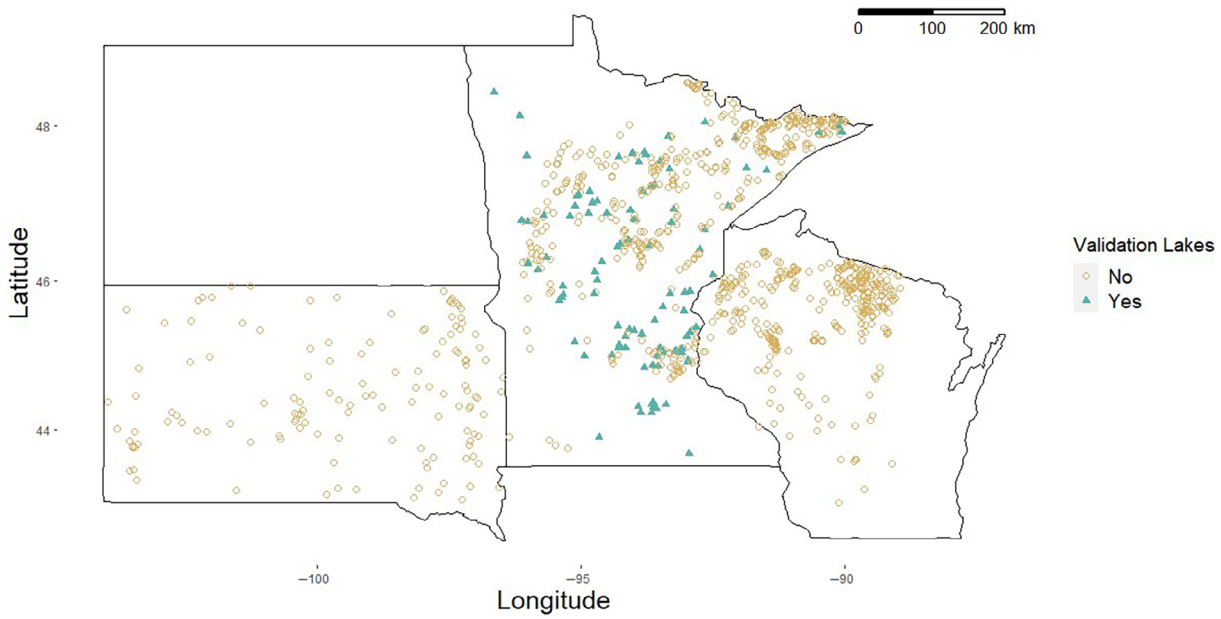

Fig. 5. Map of 1012 ImageJ digitized lakes. Turquoise closed triangles represent the 100 validation lakes, Tan open circles represent the lakes for which digitized hypsography was previously nonexistent.

Our method requires that individual users at times make subjective decisions and thus it is important to measure inter-observer reliability and reproducibility (Martin and Bateson 1993). The low values for average MAD and MSD between ImageJ processors suggest that hypsographic calculations are highly consistent between users.

The comparison of null hypsographic models and DEMs indicated the null hypsographic models are not accurate depictions of lake hypsography. The MAD of the null model vs. DEMs was consistently three times higher than the MAD of ImageJ digitizations vs. DEMs. However, we found the linear interpolation of hypsography performed much better than an ellipsoidal interpolation for hypsography and volume. In cases where no bathymetric maps exist for a lake but there is a maximum depth estimate, we suggest researchers use a linear interpolation of maximum depth.

Lake volume was found to be well represented by ImageJ, was consistent between ImageJ users, and was vastly better than null hypsographic models. Estimates of lake volume produced using ImageJ are more accurate than the null method or predictive models of lake depth (Messager et al. 2016). Global scale maximum and mean depth measurements are incredibly important for limnology. The data and methodology we provide will supplement these efforts by increasing the amount of accurate reference data that may not be available in key areas.

Our method of using ImageJ to digitize bathymetric maps allows for consistent, accurate, and efficient extraction of hypsographic data. The methods described here are supporting ongoing work to estimate thermal and optical habitat for lakes throughout the Midwestern United States but are applicable to lakes worldwide. Rapid estimation of lake morphometry has already increased the number of lakes for which temperature modeling is possible in the Midwestern United States (Fig. 5). Given the importance of lake depth for numerous limnological processes, we anticipate that this methodology will be useful for multiple applications. Any analysis that requires information on lake volume, mean depth or hypsographic curves will benefit from this method, such as landscape models of lake temperature (Rose et al. 2016; Winslow et al. 2017) or thermal-optical habitat (Lester et al. 2004; Hansen et al. 2019). Our methodology is easy to apply and accurate, and relatively time efficient. We found the time to digitize a lake using ImageJ is highly dependent on lake morphometry (lakes that have complicated morphometry take longer to digitize). For simple lakes, ImageJ can produce digitizations within a few minutes, but we estimate an average lake will take 15 min to digitize (although really complex multi-basin lakes can take much longer). We encourage others to continue this work to increase our knowledge of lake morphometry worldwide. Such applications will increase our ability to evaluate regional, national, and global patterns in lakes.

Comments and recommendations

We recommend other researchers use ImageJ for the extraction of hypsographic data when appropriate. One example of a use-case is when there are numerous undigitized bathymetric maps that are necessary for a study. Bathymetric maps are often widely available, and the potential uses of the hypsographic data contained within these maps are great. To ensure that hypsographic data derived from ImageJ are accurate, we recommend users take a similar approach as described in this work. The comparison of ImageJ-derived hypsography

with existing hypsographic data will allow for the accuracy of each user to be evaluated and ensure robust depth data.

Data availability statement

The dataset and metadata with permanent identifier are available in Rounds et al. (2022).

References

Ai, B., Z. Wen, Z. Wang, R. Wang, D. Su, C. Li, and F. Yang. 2020. Convolutional neural network to retrieve water depth in marine shallow water area from remote sensing images. IEEE J. Sel. Top. Appl. Earth Obs. Remote Sens. **13**: 2888–2898. doi:10.1109/JSTARS.2020.2993731

Algesten, G., S. Sobek, A.-K. Bergstrom, A. Agren, L. J. Tranvik, and M. Jansson. 2004. Role of lakes for organic carbon cycling in the boreal zone. Glob. Chang. Biol. **10**: 141–147. doi:10.1111/j.1365-2486.2003.00721.x

Carpenter, S. R. 1983. Lake geometry: Implications for production and sediment accretion rates. J. Theor. Biol. **105**: 273–286. doi:10.1016/S0022-5193(83)80008-3

Cross, T. K., and P. C. Jacobson. 2013. Landscape factors influencing lake phosphorus concentrations across Minnesota. Lake Reserv. Manag. **29**: 1–12. doi:10.1080/10402381.2012.754808

Dost, R. J. J., C.M. Mannaerts, and J. Dangermond (eds.). 2008. Generation of lake bathymetry using sonar, satellite imagery and GIS. Proceedings of the 2008 ESRI International User Conference: GIS, Geography in Action, Faculty of Geo-Information Science and Earth Observation. Water Resources, San Diego, Florida.

Gorham, E., and F. M. Boyce. 1989. Influence of lake surface area and depth upon thermal stratification and the depth of the summer thermocline. J. Great Lakes Res. **15**: 233–245. doi:10.1016/S0380-1330(89)71479-9

Håkanson, L. 2004. Lakes: Form and function, 1st ed. Blackburn Press.

Håkanson, L. 2005. The importance of lake morphometry and catchment characteristics in limnology—Ranking based on statistical analyses. Hydrobiologia **541**: 117–137. doi:10.1007/s10750-004-5032-7

Hansen, G. J. A., L. A. Winslow, J. S. Read, M. Treml, P. J. Schmalz, and S. R. Carpenter. 2019. Water clarity and temperature effects on walleye safe harvest: An empirical test of the safe operating space concept. Ecosphere **10**: e02737. doi:10.1002/ecs2.2737

Heathcote, A. J., P. A. del Giorgio, and Y. T. Prairie. 2015. Predicting bathymetric features of lakes from the topography of their surrounding landscape. Can. J. Fish. Aquat. Sci. **72**: 643–650. doi:10.1139/cjfas-2014-0392

Herb, W. R., L. B. Johnson, P. C. Jacobson, and H. G. Stefan. 2014. Projecting cold-water fish habitat in lakes of the glacial lakes region under changing land use and climate regimes. Can. J. Fish. Aquat. Sci. **71**: 1334–1348. doi:10.1139/cjfas-2013-0535

Hijmans, R. J., and J. van Etten. 2012. raster: Geographic analysis and modeling with raster data. R package version 2.0-12. http://CRAN.R-project.org/package=raster

Hollister, J., and W. B. Milstead. 2010. Using GIS to estimate lake volume from limited data. Lake Reserv. Manag. **26**: 194–199. doi:10.1080/07438141.2010.504321

Hollister, J. W., W. B. Milstead, and M. A. Urrutia. 2011. Predicting maximum lake depth from surrounding topography. PloS One **6**: e25764. doi:10.1371/journal.pone.0025764

Jacobson, P. C., H. G. Stefan, and D. L. Pereira. 2010. Coldwater fish oxythermal habitat in Minnesota lakes: Influence of total phosphorus, July air temperature, and relative depth. Can. J. Fish. Aquat. Sci. **67**: 2002–2013. doi:10.1139/F10-115

Kalff, J. 2002. Limnology: Inland water ecosystems. Prentice Hall.

Khazaei, B., L. K. Read, M. Casali, K. M. Sampson, and D. N. Yates. 2022. GLOBathy, the global lakes bathymetry dataset. Sci. Data **9**: 36. doi:10.1038/s41597-022-01132-9

Martin, P., and P. Bateson. 1993. Measuring behaviour: An introductory guide, 2nd ed. Cambridge Univ. Press. doi:10.1017/CBO9781139168342

Messager, M. L., B. Lehner, G. Grill, I. Nedeva, and O. Schmitt. 2016. Estimating the volume and age of water stored in global lakes using a geo-statistical approach. Nat. Commun. **7**: 13603. doi:10.1038/ncomms13603

Oliver, S. K., P. A. Soranno, C. E. Fergus, T. Wagner, L. A. Winslow, C. E. Scott, K. E. Webster, J. A. Downing, and E. H. Stanley. 2016. Prediction of lake depth across a 17-state region in the United States. Inland Waters **6**: 314–324. doi:10.1080/IW-6.3.957

Pal'shin, N. I., T. V. Efremova, and M. S. Potakhin. 2008. The effect of morphometric characteristics and geographic zonality on thermal stratification of lakes. Water Resour. **35**: 191–198. doi:10.1134/S0097807808020073

Read, J. S., L. A. Winslow, G. J. A. Hansen, J. Van Den Hoek, P. C. Hanson, L. C. Bruce, and C. D. Markfort. 2014. Simulating 2368 temperate lakes reveals weak coherence in stratification phenology. Ecol. Model. **291**: 142–150. doi:10.1016/j.ecolmodel.2014.07.029

Rose, K. C., L. A. Winslow, J. S. Read, and G. J. A. Hansen. 2016. Climate-induced warming of lakes can be either amplified or suppressed by trends in water clarity. Limnol. Oceanogr. Lett. **1**: 44–53. doi:10.1002/lol2.10027

Rounds C. Hansen G. Vitense K. Van Pelt A. 2022. Digitization of Minnesota and Wisconsin bathymetric maps resulting in hypsographic data. Data Repository for the University of Minnesota. Available from http://hdl.handle.net/11299/216182.

Rueden, C. T., J. Schindelin, M. C. Hiner, B. E. DeZonia, A. E. Walter, E. T. Arena, and K. W. Eliceiri. 2017. ImageJ2: ImageJ for the next generation of scientific image data. BMC Bioinf. **18**: 529. doi:10.1186/s12859-017-1934-z

Schwarz, R., G. Mandlburger, M. Pfennigbauer, and N. Pfeifer. 2019. Design and evaluation of a full-wave surface and

bottom-detection algorithm for LiDAR bathymetry of very shallow waters. ISPRS J. Photogramm. Remote Sens. **150**: 1–10. doi:10.1016/j.isprsjprs.2019.02.002

Sobek, S., J. Nisell, and J. Fölster. 2011. Predicting the depth and volume of lakes from map-derived parameters. Inland Waters **1**: 177–184. doi:10.5268/IW-1.3.426

Stachelek, J. 2022. glmutils: Utilities for the general lake model. R package version 0.0.0.9000.

Stachelek, J., L. K. Rodriguez, J. Díaz Vázquez, A. Hawkins, E. Phillips, A. Shoffner, I. M. McCullough, K. B. King, J. Namovich, L. A. Egedy, M. Haite, P. J. Hanly, K. E. Webster, K. S. Cheruvelil, and P. A. Soranno. 2021. LAGOS-US DEPTH v1.0: Data module of observed maximum and mean lake depths for a subset of lakes in the conterminous U.S. Environmental Data Initiative. doi:10.6073/PASTA/64DDC4D04661D9AEF4BD702DC5D8984F

Stefan, H. G., M. Hondzo, X. Fang, J. G. Eaton, and J. H. McCormick. 1996. Simulated long term temperature and dissolved oxygen characteristics of lakes in the north-central United States and associated fish habitat limits. Limnol. Oceanogr. **41**: 1124–1135. doi:10.4319/lo.1996.41.5.1124

Winslow, L. A., J. S. Read, G. J. A. Hansen, and P. C. Hanson. 2015. Small lakes show muted climate change signal in deepwater temperatures. Geophys. Res. Lett. **42**: 355–361. doi:10.1002/2014GL062325

Winslow, L. A., G. J. A. Hansen, J. S. Read, and M. Notaro. 2017. Large-scale modeled contemporary and future water temperature estimates for 10774 Midwestern U.S. lakes. Sci. Data **4**: 1–11. doi:10.1038/sdata.2017.53

Acknowledgments

The authors want to primarily thank Amanda Van Pelt for her assistance with the project. The authors thank employees of the Minnesota and Wisconsin Departments of Natural Resources for data. In particular, thanks to Andy Wilcot (MN DNR), Alex Latzka (WI DNR), Kelly Rooker, and Jordan Read (USGS). The authors also want to thank members of the Hansen lab for their comments on the manuscript. This work was funded by the Minnesota Department of Natural Resources. In addition, the authors thank two anonymous reviewers for their constructive feedback on an earlier draft of this manuscript.

Submitted 24 March 2023
Revised 30 June 2023
Accepted 06 July 2023

Associate editor: John P. Smol